Postprint of: Adamczak B., Wieczór M., Kogut M., Stangret J., Czub J., Molecular basis of the osmolyte effect on protein stability: a lesson from the mechanical unfolding of lysozyme, BIOCHEMICAL JOURNAL, Vol. 473, Iss. 20 (2016), pp. 3705-3724, DOI: 10.1042/BCJ20160604

Molecular basis of the osmolyte effect on protein stability: a lesson from the mechanical unfolding of lysozyme

Beata Adamczak*, Miłosz Wieczór*, Mateusz Kogut, Janusz Stangret and Jacek Czub

Osmolytes are a class of small organic molecules that shift the protein folding equilibrium. For this reason, they are accumulated by organisms under environmental stress and find applications in biotechnology where proteins need to be stabilized or dissolved. However, despite years of research, debate continues over the exact mechanisms underpinning the stabilizing and denaturing effect of osmolytes. Here, we simulated the mechanical denaturation of lysozyme in different solvent conditions to study the molecular mechanism by which two biologically relevant osmolytes, denaturing (urea) and stabilizing (betaine), affect the folding equilibrium. We found that urea interacts favorably with all types of residues via both hydrogen bonds and dispersion forces, and therefore accumulates in a diffuse solvation shell around the protein. This not only provides an enthalpic stabilization of the unfolded state, but also weakens the hydrophobic effect, as hydrophobic forces promote the association of urea with nonpolar residues, facilitating the unfolding. In contrast, we observed that betaine is excluded from the protein backbone and nonpolar side chains, but is accumulated near the basic residues, yielding a nonuniform distribution of betaine molecules at the protein surface. Spatially resolved solvent–protein interaction energies further suggested that betaine behaves in a ligand- rather than solvent-like manner and its exclusion from the protein surface arises mostly from the scarcity of favorable binding sites. Finally, we found that, in the presence of betaine, the reduced ability of water molecules to solvate the protein results in an additional enthalpic contribution to the betaine-induced stabilization.

Introduction

Protein folding and unfolding are fundamental processes for all living cells and as such have been extensively studied for several decades [1–4]. It is well known that multiple factors, including temperature [5], pH and pressure [6], can shift the equilibrium between the folded and unfolded states. A protein folding equilibrium can also be modulated by a class of organic co-solvents, often termed osmolytes, which are accumulated in cells in response to environmental stresses [7–9]. Osmolytes have been shown to affect the structural and thermal stability of proteins and other macromolecules [10,11], protein–protein and protein–DNA association [12] and the degree of reversibility of the folding/unfolding transition [9,11,13].

Urea, a byproduct of amino acid catabolism, is known to shift the folding equilibrium toward the unfolded state and to induce, at relatively high concentrations (>4 M), a complete protein denaturation [11,13–15]. Interestingly, even though urea disturbs protein structure and function, it is accumulated (up to ∼600 mM) as a major osmolyte in certain cells and tissues, including the mammalian kidney medulla, to balance the high osmotic pressure of the extracellular medium [7]. This is possible because the damaging effect of elevated urea on proteins in these cells is counteracted by controlled accumulation of protecting co-solvents, such as methylamines, particularly glycine betaine and trimethylamine N-oxide (TMAO), as well as sugars and other polyols [7,9,16,17]. These co-solvents, referred to as compatible osmolytes, play a key role in the adaptation of cells to hypertonicity and other stresses, as they can stabilize proteins by shifting the folding equilibrium toward the native state, generally without affecting their cellular function [7,13,14,18].

Osmolytes are also commonly used in molecular biology and biotechnology, for example, to assist the proper folding of recombinant proteins by exploiting ‘chemical chaperone’ activity of osmoprotectants such as betaine or TMAO, or to facilitate refolding and activation of proteins expressed as insoluble inclusion bodies, as in the case of urea, guanidine hydrochloride and other denaturants [7,9,19].

Despite previous efforts, the molecular underpinnings of the co-solvent-induced protein stabilization and destabilization are not yet fully established [11,13,15,20–24]. Two basic/general mechanisms, ‘direct’ and ‘indirect’, or their specific combination [10,25,26] have usually been put forward to explain the effect of osmolytes on protein stability. According to the direct mechanism, osmolytes can perturb the equilibrium between the folded and unfolded states by preferential, usually favorable interactions, such as hydrogen

bonding, with the protein surface [15,20,27–31]. On the other hand, in the indirect scenario, co-solvent molecules alter the structural and dynamic properties of water, which can lead to weakening of the protein-stabilizing hydrophobic effect or to a decrease in the overall solvation capability of the mixture [22,24,32,33]. Indeed, many osmolytes are known to disrupt or enhance the natural water structure and hence are sometimes referred to as 'structure breakers' (urea) or 'structure makers' (betaine) [34,35].

Although the indirect mechanism has been previously invoked to account for the denaturing effect of urea [36,37], it is now more commonly believed that urea induces unfolding by interacting with a protein more strongly than with water, that is, by stabilizing the unfolded state in which the protein surface accessible for direct interactions with the solvent is larger [11,13,28,30,38–40]. The molecular mechanism behind this preferential interaction is, however, less clear. Recent data, obtained by measuring the transfer free energies of side chain and backbone units between water and urea solution [39,41] and by hydrogen-exchange experiments [38], suggest that the main enthalpic driving force for the urea-induced unfolding is provided by direct interactions between urea and the protein backbone. In contrast, preferential interactions of urea with model compounds determined by osmometry indicate that interactions with the protein side chains are at least equally important, contributing 60% to the total effect of urea [42]. This finding is also consistent with the molar volume and compressibility data for amino acids in urea solution [29] and with recent molecular dynamics simulations [13,28,30]. The observed propensity of urea to bind to the protein surface has been explained either by its ability to form hydrogen bonds — particularly with the backbone amide and carbonyl groups [38] — or by favorable dispersion interactions, mostly with the protein side chains [23,27,28,43].

Even less clear is the mechanism by which betaine and other methylamines shift the folding equilibrium toward the protein native state. According to the prevailing model, based largely on osmometry and transfer free energy measurements [39,40,42,44,45], the protecting co-solvents are preferentially excluded from the surface of the protein, especially from the vicinity of the backbone peptide groups [13,18,39,40,42,44,45]. This in turn gives rise to a force opposing the protein unfolding, as in the unfolded state it is more difficult for the (effectively repelled) co-solvent to avoid the unfavorable contact with the protein surface. Therefore, in the surface exclusion model, compatible osmolytes act as crowding agents by favoring more compact protein structures typical for the native state [46–48]. This also explains why the accumulation of protein-stabilizing osmolytes can sometimes be detrimental. For example, it has been shown that by promoting compaction, protecting osmolytes can induce aggregation of unstructured proteins [17,49]; they can also impair the functioning of certain enzymes, probably by restricting their conformational flexibility [50].

Importantly, while the standard Asakura-Oosawa model based on hard-core steric interaction predicted the excluded volume-induced stabilization to be entirely entropic in nature [51], recent theoretical considerations led to the development of a more sophisticated 'soft-core' model involving both entropic and enthalpic contributions to the stabilization free energy [52,53]. In this description, the overall nature of the stabilizing depletion force depends on the respective enthalpic and entropic components of the effective protein–co-solvent interaction potential. This idea sheds new light on the results of recent circular dichroism and computational studies, which have indicated that protein stabilization by protecting osmolytes is indeed at least partially enthalpy-driven and that this contribution might be mediated by water molecules perturbed by the co-solvent [46,54,55]. This perturbation can also be linked to enhanced water ordering, an effect reported in many previous studies and often put forward to explain the effective co-solvent–solute repulsion [20,34,35,56].

Here, we used molecular dynamics simulations to identify the mechanisms by which the presence of two different co-solvents, urea and betaine, affects the stability of the tertiary structure of lysozyme, a typical globular protein used in folding studies [57]. To provide a controllable model of protein denaturation, a mechanical force was used to increase the effective radius of a lysozyme molecule, enabling us to study the native state stability by relating the expended work to the extent of unfolding along a single conformational co-ordinate. The results of the simulations were found to be in general agreement with the available experimental data on the protein–osmolyte solutions. Encouraged by this agreement, we verified

and extended the existing models of osmolyte–protein interactions to present a consistent description of the atomistic-level driving forces that govern co-solvent exclusion and accumulation.

In particular, we observed that urea interacts favorably with almost all kinds of chemical moieties at the protein surface, and that this leads to its accumulation in an extended solvation shell around the protein molecule. Importantly, we noted that hydrogen bonding alone does not account adequately for protein–urea association, and that the dispersion interactions and water-mediated hydrophobic forces are crucial for the observed accumulation and, consequently, for driving denaturation in urea solutions. Our results also indicate that betaine is preferentially excluded from the vicinity of the protein backbone, giving rise to a sequence-independent penalty for the protein unfolding. Interaction energy decomposition suggests that this exclusion at least partially stems from the ligand-like behavior of betaine at the protein surface, providing us with a molecular-level interpretation of the major entropic contribution to the depletion force that promotes protein compaction, and a possible refinement of the canonical hard-sphere model of co-solvent exclusion. Finally, we note that, in the presence of betaine, the protein–water interactions are considerably weakened, and propose that the resulting decrease in protein solvation may account for the enthalpic contribution to the stabilizing effect of betaine.

Experimental

Seven primary systems were constructed to simulate the mechanical unfolding of lysozyme in pure water and in the presence of urea and betaine. In each system, a dodecahedron simulation box with a box vector length of 7.8 nm (corresponding to ~335 nm^3) contained a single lysozyme molecule and solvent molecules corresponding to three betaine concentrations (1.0, 2.5 and 5.0 M), three urea concentrations (3.5, 5.0 and 7.0 M) and pure water (0 M). The specific numbers of water and osmolyte molecules are given in Supplementary Table S1. The force field parameters for urea, N,N^0-dimethylurea and sarcosine (N-methylglycine) were obtained from the CHARMM General Force Field (CGenFF) [58], and the parameters for betaine were obtained by analogy using the CHARMM27 parameters for phosphatidylcholine (for the trimethylammonium and methylene groups) and for phosphatidylserine (for the carboxyl group) [59]. The choice of parameters for betaine was validated against the experimentally measured m-value, preferential hydration coefficient and osmotic pressure, and satisfactory agreement was obtained, as described in detail in Supplementary Figure S1 and Table S2 [45,55,60]. For water, the TIP3P [61] model was used. The initial structure of lysozyme was taken from the X-ray structure (PDB code: 1AKI), and the CHARMM27 force field [62] was used for the protein residues.

All MD simulations were performed with the GROMACS package [63]. Periodic boundary conditions were applied, and the particle mesh Ewald (PME) method [64,65] with a real-space cutoff of 1 nm was used to account for long-range electrostatics. The simulations were carried out in the NPT ensemble using a Berendsen-type temperature coupling [66] with a coupling coefficient of 0.1 ps and a reference temperature of 300 K, and Berendsen-type pressure coupling [66] maintaining the pressure at 1 bar with a coupling coefficient of 1 ps. During the simulations, bond lengths were constrained using the LINCS algorithm [67], and a typical time step of 2 fs was used. Initially, each system was equilibrated by carrying out 1 ms unconstrained simulations.

To unfold lysozyme in a controllable manner, an external potential was then applied to the radius of gyration (R_{gyr}), defined for the reference group consisting of each C_α atom in the protein backbone:

$$R_{\mathrm{gyr}} = \sqrt{\frac{1}{N}\sum_{C_\alpha} (\boldsymbol{r}_i - \boldsymbol{r}_{\mathrm{COM}})^2}, \quad (1)$$

where N is the number of C_α atoms, r_i is the position of ith C_α atom and r_{COM} is the position of the center of mass of the reference group.

During the enforced unfolding, R_{gyr} was changed from the initial value of 1.4 nm in the native state up to 3.0 nm, with a harmonic force constant of 7000 kJ mol^{-1} nm^{-2}, and four pulling speeds were used: 1 × 10^{-4}, 1 ×

10^{-5}, 5×10^{-5} and 5×10^{-6} nm ps^{-1}. To improve the signal-to-noise ratio in the unfolding curves, five simulation runs were carried out for each system at the lowest pulling speed.

Systems with 2.5 M sarcosine, 5 M N,N^0-dimethylurea and 5 M scaled-charge betaine were prepared in an analogous manner, and only the lowest pulling speed of 5×10^{-6} nm ps^{-1} was used. In the charge scaling simulations, all partial charges of the betaine molecule were scaled by a common factor of 1.2, 1.4 or 1.6. The total simulation time for data collection was 51 ms. In the hydrogen bond analysis, H-bonds were identified based on a donor–acceptor distance criterion of 0.35 nm and a 40° threshold for the hydrogen-donor–acceptor angle. Average H-bond energies were estimated using the formula by Espinosa et al. [68]:

$$E_{HB} = 2.5 \times 10^4 \exp(-36d(\mathrm{H}\ldots\mathrm{O})) \quad (2)$$

where d(H ... O) is the hydrogen-acceptor distance in nm and E_{HB} is the H-bond energy in kJ/mol.

Results and discussion

A common pathway of the enforced unfolding

To investigate the effect of typical denaturing and protecting osmolytes on the stability of the protein native state, we used nonequilibrium molecular dynamics to simulate mechanical unfolding of lysozyme in pure water and in the presence of increasing concentrations of urea and betaine. To this end, external steering forces were applied to all C_α atoms of the protein to increase its radius of gyration, R_{gyr}, from the initial value of 1.4 nm, characteristic of the native state, to a threshold value, in each case set at 3.0 nm (see Experimental for details).

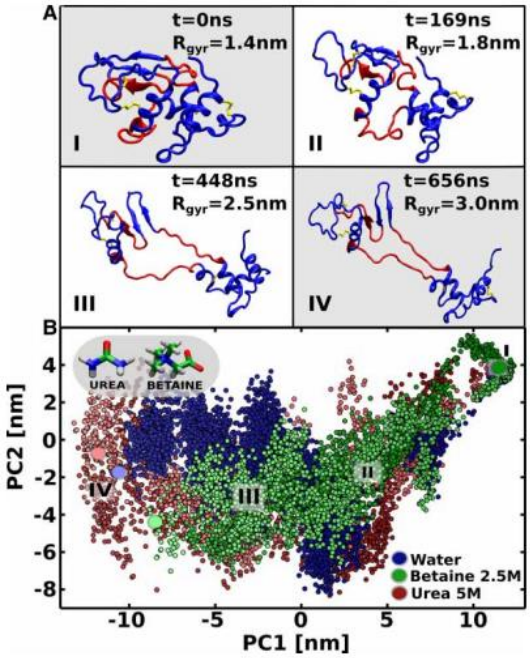

Figure 1. The mechanical unfolding of lysozyme.
(**A**) Snapshots of the simulated unfolding pathway obtained at the pulling speed of 5×10^{-6} nm ps^{-1}. The values of the radius of gyration in consecutive snapshots are: 1.4 nm — the native state; 1.8 nm — a rupture point; 2.0 nm — large changes in the lysozyme structure, i.e. the previously buried protein portion marked in red becomes exposed to the solvent; 3.0 nm — an arbitrary final state. (**B**) Unfolding trajectories in pure water (blue), in the presence of betaine (green) and in the presence of urea (red) projected onto the reduced subspace defined by the first two eigenvectors extracted from the unfolding in pure water. The initial and the final states are shown as large circles. All molecular images were created using VMD [69].

Inspection of the resulting trajectories shows that for all systems the unfolding process, illustrated in Figure 1A, follows a common pathway: the protein splits into two globular subdomains, each held together by two disulfide bonds, and interconnected by two antiparallel, extended strands that upon unfolding become exposed to the solvent. To examine if this folded-to-unfolded conformational transition depends on the solvent composition, we projected the trajectories for all systems onto the plane formed by two first principal co-ordinates (PCs) obtained for the unfolding in pure water using principal component analysis. Figure 1B combines three such projections, depicting the unfolding pathways in pure water, 5.0 M urea and in 2.5 M betaine. As can be seen, in this projection the mechanically induced unfolded state of lysozyme in water (blue circle in Figure 1B) corresponds well to the endpoints of the respective unfolding pathways in urea and betaine solutions (red circle and green circle, respectively, in Figure 1B). As the first PCs by construction capture the large-scale unfolding modes, the proximity of the end-state projections suggests that, irrespective of the solvent composition, lysozyme evolves along a common enforced unfolding pathway adopting similar final structures. This conclusion finds further support in the dependence of the lysozyme solvent accessible surface area (SASA) and root-mean-square deviation on the radius of gyration, as shown in Supplementary Figures S2 and S3, respectively.

Work of unfolding provides a measure of the co-solvent-induced equilibrium shift

The force–extension curves (the steering force vs. R_{gyr}), shown in Figure 2A, reveal that lysozyme unfolds in an apparent two-state fashion with one dominant activation barrier that is effectively lowered by the applied potential. Initially, up to the rupture point (R_{gyr}≈ 1.7 nm), which is relatively insensitive to the solvent composition, we observe a linear elastic response of the lysozyme molecule, with the structural deformation increasing proportionally to the applied force. The high energetic cost of the lysozyme unfolding during this initial stage is largely due to exposure of formerly buried hydrophobic side chains and other nonpolar segments to the solvent, as indicated by a large change in SASA (Supplementary Figure S2). After the rate-limiting barrier is overcome, the further increase in SASA is less pronounced and the steering force drops abruptly to much lower positive values, although the effect of high concentrations of urea and betaine, facilitating or opposing the unfolding, is still noticeable.

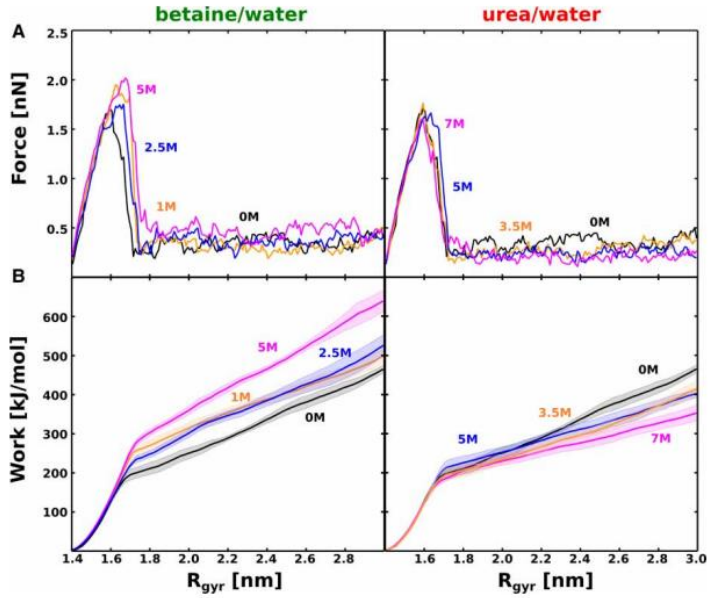

Figure 2. Pulling forces and unfolding work in steered MD simulations.
(**A**) The force–extension profiles for the lysozyme unfolding in the presence of increasing concentration of betaine and urea. (**B**) The corresponding profiles of unfolding work as a function of R_{gyr}. All data correspond to the pulling speed of 5×10^{-6} nm ps^{-1}; for higher pulling speeds, see Supplementary Figures S4 and S5. All values were averaged over five independent simulations, with the shaded area representing the standard error of the estimate.

Figure 2B shows the amount of work required to unfold lysozyme in the presence of both co-solvents and in pure water, obtained at the lowest pulling speed of 5×10^{-6} nm ps^{-1} by integrating the steering force over R_{gyr} from the initial value up to 3 nm. Given the similar energy dissipation, the differences in the unfolding work with respect to pure water can be expected to reflect the actual perturbing effect of co-solvents on the protein folding equilibrium. Indeed, we found that, compared with pure water, more work is needed to unfold the lysozyme in the presence of betaine, by up to 40% with a 5.0 M solution, and the opposite is the case for the urea solutions, i.e. lysozyme becomes more susceptible to mechanical stress with the unfolding work decreasing by up to 20% with a 7.0 M urea solution. Therefore, these results indicate that the unfolding work computed using our model consistently captures the well-known fact that betaine stabilizes the native protein structure, while urea acts as a denaturing agent. It is, however, necessary to remark here that the value of the unfolding work itself — obtained with pulling speed orders of magnitude higher than in actual single-molecule experiments [70,71] — cannot be directly compared with the free energy of unfolding, as the expended work approaches free energy only in the quasi-static limit. Interestingly, in both osmolyte solutions, the expended work increases faster with increase in the pulling speed than in pure water such that the destabilizing effect of urea is effectively reversed in the limit of fast unfolding (Supplementary Figure S4). As both betaine and urea solutions have higher viscosity than pure water [72,73], this tendency suggests that whereas at higher speeds the steering force is dominated by viscous drag, at the lowest speed, the dissipation is small enough for the calculated work to reflect the osmolyte-induced effect on the folding equilibrium. It is worth noting that reduction in nonequilibrium effects is also seen from the increase in the number of H-bonds between the protein and urea with decrease in pulling speeds (see Supplementary Figure S5).

We additionally tested the above conclusions by performing simulations of forced unfolding of lysozyme in the presence of two other similar osmolytes, sarcosine (N-methylglycine) and N,N^0-dimethylurea. The former stabilizes proteins more efficiently than betaine while having a slightly lower viscosity, and the latter is a more effective denaturant than urea while also being more viscous [72–74]. The unfolding work, shown in Supplementary Figure S6, is smaller in N,N^0-dimethylurea than in urea solution, and larger in sarcosine than in betaine solution, consistent with the prevailing effect of osmolyte-induced (de-)stabilization and not with a dominating impact of solvent viscosity.

Hydrogen-bonding analysis reveals major differences between unfolding in urea and betaine solutions

It is expected that with increase in co-solvent concentrations, the amount of water available to solvate the hydrogen-bonding sites of the protein decreases in both the folded and unfolded state. Hydrophilic osmolyte molecules may compensate for this decrease by providing additional hydrogen bonds with the protein. However, co-solvents have different H-bonding properties compared with water, and such differences in solvation properties lead to positive or negative enthalpies of transfer of a protein from water to the osmolyte solution. Since the number of H-bonding sites on the protein surface generally increases during unfolding, these non-zero transfer enthalpies may contribute to stabilization or destabilization of the native state, respectively.
Accordingly, we determined the number of H-bonds formed between lysozyme and the solvent components as a function of the unfolding coordinate R_{gyr} (Figure 3A). Since the work of unfolding in each system relates to the differences in the number of H-bonds between the unfolded and folded states rather than the absolute numbers, in Figure 3B, we also compared the overall changes observed.

To make our results less sensitive to the conformational fluctuations of the numerous charged side chains on the protein surface, we focused the H-bonding analysis on the two antiparallel strands (Glu35–Asn65 and Ile88–Ala110) connecting the two lysozyme subdomains that split apart during the unfolding (Figure 1). To further facilitate the comparison, the intervening β-hairpin (Thr43–Gly54) responding differently in the betaine and urea solutions has been excluded. The chosen fragments, referred to as ‘exposed’ and shown

in red in Figure 1, are continuous polypeptide chains representative of the regions that are buried in the folded proteins and become exposed upon unfolding.

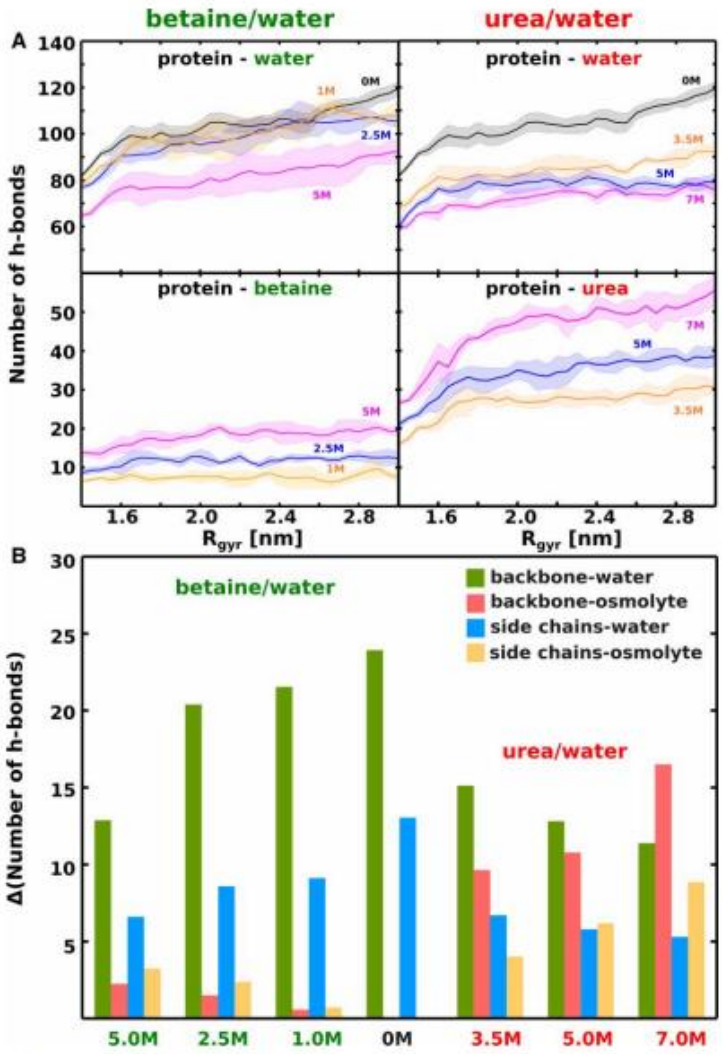

Figure 3. Unfolding-induced changes in hydrogen bonding.

(**A**) Number of hydrogen bonds formed between the protein and the co-solvent or water molecules during the unfolding as a function of R_{gyr}. (**B**) The increase in the number of hydrogen bonds upon unfolding of lysozyme in pure water and in the presence of osmolytes. Four contributions are shown: backbone — water (green), backbone — osmolyte (red), side chains — water (blue), side chains — osmolyte (orange). All data correspond to the lowest pulling speed (5×10^{-6} nm ps^{-1}). All values were averaged over five independent simulations, with the shaded area representing the standard error of the estimate.

It can be seen from the left panels of Figure 3A that over the entire range of R_{gyr}, the total number of protein–water H-bonds in the betaine solution is only slightly reduced relative to that found in pure water (by up to 20% for the highest betaine concentration). At the same time, even though betaine can potentially form H-bonds with the protein via the carboxyl group, the number of such bonds remains relatively low during the unfolding. In fact, Figure 3B shows that the increase in the number of H-bonds formed by the protein with water is much larger than that with betaine and is also comparable with that seen in the absence of osmolytes, especially for the protein backbone for which 80–90% of the corresponding increase in pure water is observed. This reveals that the newly exposed H-bonding sites are solvated preferentially by water molecules and suggests that betaine is excluded from residues that form the protein core, in agreement with the experimental data [18,39,40,44,45].

The volume associated with unfavorable protein–co-solvent interactions — roughly proportional to the surface area — introduces a penalty for unfolding, as the solvent-exposed surface area is typically larger in the unfolded state; hence, exclusion from the protein surface has been suggested to account for the stabilizing effect of protecting co-solvents. The exclusion itself can basically occur through two main mechanisms. In the first scenario, betaine is excluded from protein surfaces by the effective repulsion, which may result either from the preference of a protein to interact with water or from the fact that incorporation of a bulky and highly polar betaine molecule into the protein surface requires satisfying certain steric and electrostatic constraints. Alternatively, since hydrogen bonds were found to be markedly shortened in the solvation shell of betaine [74,75], the exclusion effect can be ascribed to a strongly bound hydration layer that presumably forms around the osmolyte and reduces its interactions with the protein surface.

In stark contrast with betaine, the right panels of Figure 3 show that in urea solutions, it is the osmolyte that preferentially solvates the exposed H-bonding sites on the protein. Despite the fact that water molecules outnumber urea molecules by 4.5- to 12-fold, Figure 3B reveals that the number of new protein–urea H-bonds is comparable with that of protein–water (70–130% of the latter depending on the urea concentration). This suggests that urea interacts with the initially buried residues more favorably than water, and is significantly enriched at the protein surface, as observed experimentally [39,40,42,76]. The preferential protein–urea interactions overcompensate the entropy loss due to the urea/water concentration gradient and, therefore, are commonly believed to be responsible for the denaturing effect of urea [15,30,77,78]. The exact molecular mechanism of this preferential accumulation is, however, less clear [13,76].

In addressing this question, we first note that the increase in the total number of H-bonds between the protein and the solvent is only slightly greater (average by 3%) in the urea solution than in pure water (Figure 3). If we also take into account that the H-bonds formed by urea with the protein are on average longer and hence energetically less favorable than those formed by water (by ~10 kcal/mol, averaging over all concentrations employed), as shown by the H-bond energy analysis in Supplementary Figure S7 and Table S3, it can be concluded that, in urea solutions, direct H-bonds tend to stabilize unfolded protein conformations even less efficiently than in pure water. Therefore, contrary to some previous reports [26,38,79], H-bonding (polar) interactions alone are not sufficient to account for the reduced work of unfolding in urea solutions. Apparently, urea-induced destabilization occurs primarily due to nonpolar interactions including, as previously suggested, favorable urea–protein dispersion interactions [20,28,43] and/or weakening of the hydrophobic effect by urea accumulated at the protein surface [27,36,77,80].

To further verify this conclusion, we extracted representative structures from the unfolded ensemble generated in 5.0 M urea, replaced the co-solvent with water and ran 100 ns MD simulations with the backbone atoms positionally restrained; the reverse procedure, i.e. ‘resolvation’ of the unfolded conformations generated in pure water with 5.0 M urea was also carried out (with all solvent molecules added anew in both cases). Changes in the H-bonding pattern upon solvent exchange, summarized in Supplementary Table S4, show that, in the presence of urea, the number of protein–solvent H-bonds is larger by only 2–3%, regardless of the protein conformation and a particular unfolding pathway. This result confirms that the overall ability of pure water to saturate the exposed H-bonding sites is very similar to that of urea solutions. Furthermore, the distribution of the total number of H-bonds between various types of residues is also quite similar for both solvents (with differences in the range of 0–7%).

Previous works have proposed that the effect of betaine and other methylamines on protein stability is partially enthalpic in origin and that it may stem from decreased protein solvation [46,52,53,55,81]. Accordingly, our data presented in Figure 3B show that the total number of new H-bonds, i.e. water–protein and betaine– protein combined, in the betaine solutions is reduced by ~10% compared with pure water, with no apparent dependence on betaine concentration. This decrease — leading to a less favorable solvation energy of the unfolded state — might be thought to account for the enthalpic cost of the unfolding in betaine solutions. To more directly test whether betaine solutions indeed have lower ability to solvate the exposed polar groups of the protein, we carried out for betaine an analogous ‘resolvation’ procedure to that

described above for urea. We found (Supplementary Table S5) that, upon betaine addition, the number of H-bonds between the solvent and the backbone of the lysozyme unfolded in pure water decreases by ~10%, with almost all bonds (93.80%) formed by water molecules and the osmolyte contributing the remaining 2.20%. A similar decrease in the number of H-bonds is seen for the polar (6%) and hydrophobic (11%) side chains, while preferential H-bonding between betaine and positively charged basic residues partially compensates for this desolvation. These observations suggest that betaine present as a co-solvent measurably reduces the water activity, thereby disfavoring water–protein H-bonds. Since betaine itself is largely excluded from the vicinity of the protein and, therefore, cannot fully compensate for the loss of water–protein H-bonds, the resulting desolvation may possibly lead to enthalpic destabilization of the unfolded state with respect to the native one. It should be noted, however, that because H-bonds involving betaine are generally shorter (and thus stronger) than those involving water (Supplementary Figure S7 and Table S3), the overall destabilization effect can be less pronounced than would be expected from simple H-bond counting. Indeed, correcting for differences in average energy of H-bonds formed by water and betaine results in total H-bond energy changes that are only slightly (7–30 kcal/ mol) smaller in high betaine concentrations than in pure water.

Betaine exclusion as a local and urea accumulation as a more general phenomenon

Prompted by the nonuniform distribution of the solvent components around the protein, seen already in the H-bond analysis, we computed the local-bulk partition coefficient to provide a more detailed picture of the exclusion and accumulation phenomena at the protein surface. The coefficient reflects the deviation from a uniform spatial distribution of co-solvent molecules in the vicinity of the solute and was defined as follows:

$$K_{\mathrm{p}} = \frac{N_{\mathrm{o}}}{N_{\mathrm{w}}} \frac{N_{\mathrm{w}}^{\mathrm{b}}}{N_{\mathrm{o}}^{\mathrm{b}}} \tag{3}$$

with N_o and N_w being the number of osmolyte and water molecules within a defined distance from the solute (here taken to be 0.55 nm) [82], and N_o^b and N_w^b being the number of osmolyte and water molecules in bulk solvent. A value of 1 indicates equal concentrations of the osmolyte in the protein solvation shell and in bulk solvent, whereas values higher and lower than 1 correspond to enrichment and exclusion of the osmolyte from the vicinity of protein surface, respectively.
Figure 4 compares the changes in the coefficient during unfolding, computed separately for the backbone and side chains of the exposed part of the protein.

It can be seen that betaine and urea differ vastly in terms of their preference for the exposed backbone, consistent with the view that prevails in the literature [30,39,40,83]. Namely, in the solvation shell of the backbone, the fraction of urea molecules is ~1.5- (in the folded state) to 2-fold (in the unfolded state) higher compared with bulk solvent, while the concentration of betaine decreases by up to 50%.

The differences are smaller in the environment around the side chains, with the urea content ~1.5 times higher than in the bulk, and the preferential interaction coefficient is roughly equal to 1.0 for betaine in all cases. This suggests that the exclusion observed for betaine arises only locally, that is, close to the backbone, while the accumulation of urea — albeit highest at the backbone — also extends into the side chain region. Notably, osmometric measurements reported recently for betaine and similar osmoprotectants (TMAO and sarcosine) also point to the conclusion that the stabilizing effect of osmolytes is due to their exclusion from the protein backbone rather than from the side chains [39,40,44,45,83]. Figure 4 also reveals that during the course of unfolding, and in particular close to the rupture point at 1.7 nm, urea becomes more abundant at the protein surface, as the preferential interaction coefficient is greater by ~0.5 for the unfolded than for the folded lysozyme. Betaine behaves differently, as the coefficient remains roughly constant during the folded–unfolded transition. These tendencies indicate that while urea has an even

stronger preference for the regions that become exposed to solvent upon unfolding — most notably, the backbone and hydrophobic side chains — betaine exhibits similar preference for the folded and unfolded ensemble. In the case of urea, the enrichment is then amplified by an increase in solvent-exposed surface area during protein unfolding.

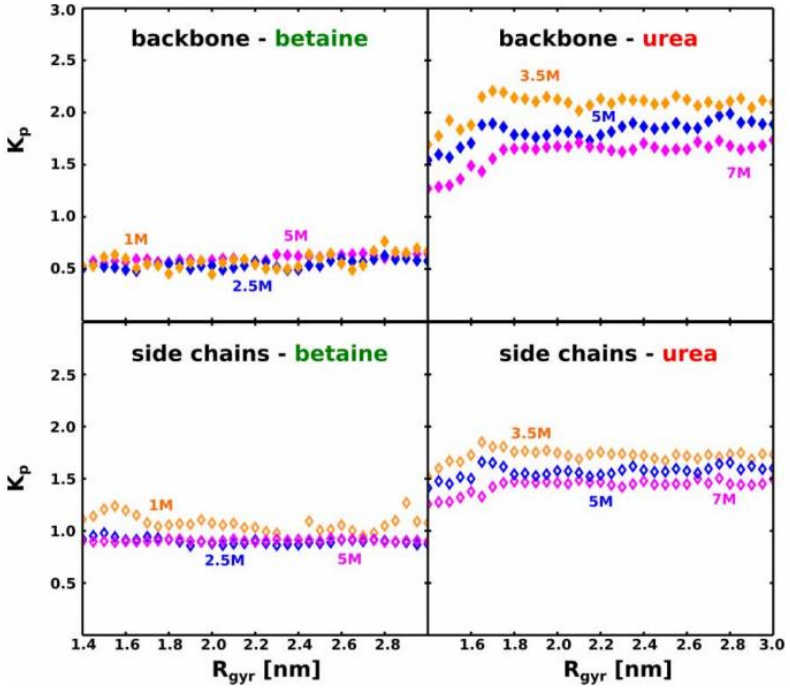

Figure 4. Analysis of exclusion and accumulation of osmolytes at the protein–solvent interface.
The local-bulk partition coefficient was calculated for the solvent molecules with respect to the protein (backbone and side chains) as a function of R_{gyr}, in different urea and betaine concentrations. All values were averaged over five independent simulations.

Since the popular approach to discuss osmolyte effects in terms of contributions from backbone and side chains [27,30,39–41] can be ambiguous due to the diverse chemical nature of the latter, we additionally dissected individual contributions from basic (b), acidic (a), polar (p), hydrophobic aromatic (h. ar) and hydrophobic aliphatic (h. al) residues to the overall K_p. This approach further facilitated a comparison of our results with available experimental and computational data [42,84–86]. Values of K_p determined for the folded and unfolded state are reported in Supplementary Table S6. Consistent with previous observations, urea accumulates at the protein surface, giving rise to K_p much larger than one. Strong urea enrichment is observed especially in the proximity of the backbone (K_p in the range of 1.44–1.90 for the folded state) and hydrophobic amino acids (K_p = 1.44–1.90). A slightly lower accumulation of urea can be seen in the vicinity of polar (K_p = 1.34–1.73) and basic (K_p = 1.31–1.63) residues, with the solvation shell of acidic side chains being the least enriched in urea (K_p = 1.11–1.46). Note that K_p values markedly larger than 1 typically decrease with concentration, as regions with high preference for urea saturate already at low concentrations, and the amount of co-solvent in their solvation shells does not change significantly with increase in bulk concentration.

On the other hand, interactions of betaine with the protein surface are mostly unfavorable ($K_p < 1$), with an exception of basic residues that were found to attract betaine molecules quite strongly (K_p = 1.23–1.96). Among other individual residue types, betaine is strongly excluded from the backbone (K_p = 0.62–0.83), hydrophobic (K_p = 0.68–0.79) and acidic (K_p = 0.75–0.84) residues, and roughly indifferent to the presence of polar side chains (K_p = 0.86–0.94).

Notably, the K_p values for urea are in good qualitative agreement with a recent report by Holehouse et al. [86], where the action of denaturants was simulated in the context of small protein domains, even though the study used different force field parameters for urea (OPLS) from those in our case (CHARMM). Such

consistency indicates that the observed behavior of urea is relatively insensitive to the choice of force field. In turn, a comparison with the experimental data of Record and colleagues [42,84,85] reveals a substantial systematic offset in the computed values — most probably due to methodological differences, as the reference study used isolated small molecules to infer values of K_p for individual atom types, and the assumed additivity need not hold for a diverse environment of the protein surface. One significant outlier is the aromatic nonpolar side chains, which were found to strongly attract betaine molecules in the reference study (K_p of 1.62), while effectively repelling betaine in our simulations (K_p of ~0.75). We note that, even though the large discrepancy can be partially explained in terms of nonadditivity (in the unfolded state, the more isolated aromatic residues have larger K_p of up to 1.03), it is possible that existing nonpolarizable atomistic models do not describe the attractive nature of, for example, cation–π interactions sufficiently well. One would need to resort to ab initio explicitsolvent models to rectify this issue.

To spatially resolve the observed interaction preferences, we calculated the radial preference function of osmolyte molecules around the unfolded state of lysozyme, for the whole protein, as well as separately for the backbone and side chains. The radial preference function was defined as the ratio of osmolyte and water molecules found at a distance r from the protein surface, divided by the corresponding ratio in the bulk solvent, according to a formula analogous to eqn (3):

$$f_o(r) = \frac{N_o(r)}{N_w(r)} \frac{N_w^b}{N_o^b} \tag{4}$$

Thus, by construction, deviations from unity in the preference function can be interpreted in the same way as for the preferential interaction coefficient. Also, to investigate the exclusion and accumulation in the vicinity of different amino acid types, we calculated the preference function separately for acidic, basic, hydrophobic and polar residues in the intermediate osmolyte concentrations, that is, in 2.5 M betaine and 5.0 M urea solutions.

As seen in Figure 5, and consistent with the above discussion, betaine molecules are excluded from the exposed backbone. Within 0.5 nm of the backbone, the concentration of betaine is ~2 times lower compared with the bulk solvent, at least in 1.0 and 2.5 M solutions. The exclusion effect is least pronounced for the 5.0 M solution, indicating that, at higher concentrations, betaine has a stronger tendency to distribute more uniformly, possibly due to overlapping of the solvation shells of betaine molecules.

On the other hand, betaine molecules approach the exposed side chains easily, forming favorable contacts at two distinct intermolecular distances that correspond to two main modes of betaine–protein interaction, seen as peaks in Figure 5C. As the decomposed distributions suggest (Figure 5D), the highest peak at 0.3–0.4 nm almost exclusively corresponds to direct salt bridges between the carboxyl moiety of betaine and side chains of basic residues. Similarly, the second, much smaller peak at 0.5–0.6 nm can be largely attributed to the direct charge–charge interaction between the trimethylammonium group of betaine and acidic residues. Owing to the three methyl groups on the nitrogen atom of trimethylammonium, in this ionic pair, the positive charge is more delocalized and separated from the negative ion and hence, the interaction is significantly weaker. Interestingly, while the distribution for polar residues has two peaks that coincide with those for charged side chains, their height suggests that, in contrast with charged side chains, polar side chains (similar to hydrophobic) cannot attract and reorient betaine molecules efficiently. This, in turn, indicates a region-specific and strongly sequence-dependent orientational distribution of betaine at the surface of the unfolded protein, suggesting also that relatively few binding sites on the protein can accommodate a betaine molecule in an enthalpically favorable manner. As proposed above, this scarcity of osmolyte-binding sites could result in effective exclusion of betaine from the vicinity of the backbone, even though, occasionally, betaine–backbone association may be enthalpically favorable (see the Discussion of decomposed interaction energetics below).

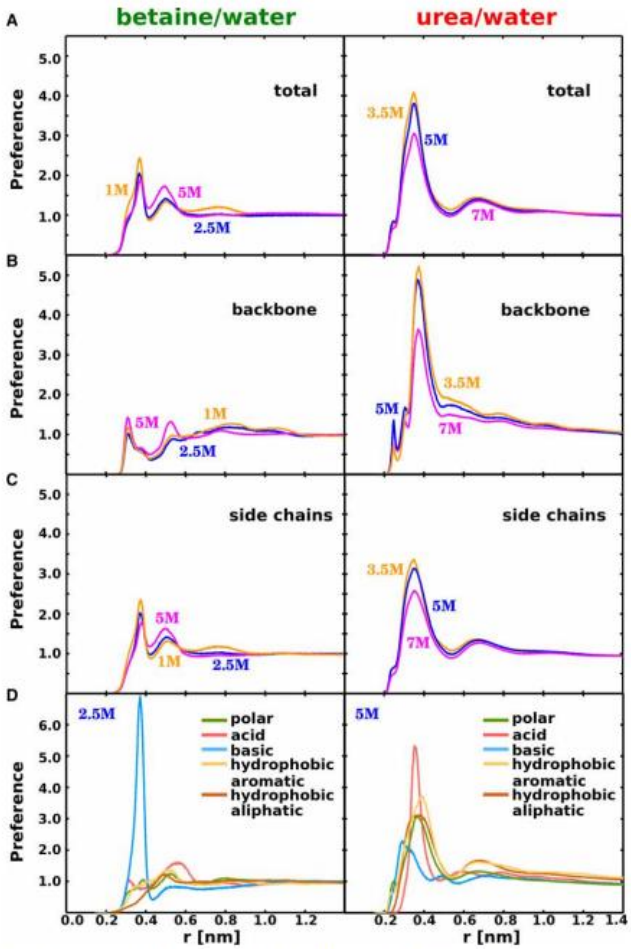

Figure 5. Radial preference functions of betaine and urea with respect to the protein.
Radial preference functions were calculated with respect to: (**A**) the whole protein molecule, (**B**) protein backbone and (**C**) protein side chains. (**D**) Radial preference functions decomposed into contributions from: polar (green), acid (red), basic (blue) and hydrophobic aromatic (orange) and hydrophobic aliphatic (brown) side chains in the intermediate osmolyte concentrations. In the chosen concentrations, betaine and urea occupy comparable volume fractions of the solvent.

Unlike betaine, urea strongly accumulates in the vicinity of the protein (Figure 5, right). Consistent with the already discussed hydrogen-bonding patterns, the urea is strongly attracted toward the backbone (local concentrations up to 3.5–5.0 times higher than in the bulk), and the enrichment is only slightly lower (up to 2.5–3.5 times) close to the side chains. Also, the peaks in the distribution functions are broader than in the case of betaine, indicating less constrained binding, i.e. protein-bound urea can assume more orientations than proteinbound betaine. Multiple factors contribute to the urea orientational and positional flexibility at the protein surface, as illustrated by the decomposed distributions in Figure 5D. For basic residues, the broader distribution reflects the possibility of forming a hydrogen bond to the charged head group and/or a hydrophobic contact with the aliphatic part of the side chain. On the other hand, the sharper and higher peak seen for acidic side chains is attributed to the fact that they interact with urea exclusively through hydrogen bonding, which, however, is entropically favored due to eight distinct ways of pairing two oxygen atoms of a carboxylic group with four hydrogen atoms of urea. The broad peak found for polar residues indicates that all kinds of donor– acceptor pairs and less specific contacts are formed in this case, which also contributes to the orientational freedom of urea at the protein–solvent interface. Finally, abundant contacts exist between urea and hydrophobic side chains, and these are nonspecific and spatially heterogeneous by nature, as confirmed again by the width of the distribution. In general, well-defined and wide peaks for uncharged residues (especially hydrophobic ones) indicate that urea indeed has a preference for the residues that form the core of the protein, as remarked above.

In the above discussion, we mentioned two potential mechanisms that relate the observed contact preference to the denaturing effect of urea: one based on weakening of the hydrophobic effect that drives protein folding [21,87,88], and another in which urea stabilizes the unfolded state by interacting favorably with the exposed protein core via van der Waals' forces [27–29,89]. Intriguingly, the distributions in Figure 5 show a decreasing but significant enrichment of urea that persists up to 1 nm from the protein surface, which suggests a picture of a diffuse urea-enriched region that surrounds the lysozyme molecule. One might expect this urea-rich shell to reduce water-mediated hydrophobic attraction between nonpolar protein surfaces, as the shell provides a local environment where water, urea and hydrophobic residues can favorably interact with each other. This supports the mechanism based on decreased hydrophobic forces; however, the other scenario, involving favorable protein–urea dispersion interaction, can still hold true, as they are not mutually exclusive and can in fact act synergistically in causing protein denaturation.

As also evident from Figure 5, at a given distance from the protein, the radial preference function can either increase or decrease with the osmolyte concentration. An increasing trend observed for certain regions of the protein surface means that, at low osmolyte concentrations, these regions are not readily solvated by the osmolyte, and the preference increases with increase in the bulk osmolyte concentration.

The regions that give rise to such an increasing trend have relatively low affinity for the osmolyte, and in the case of betaine, this corresponds almost to the entire protein surface — both the protein backbone and nonbasic side chains (as can be seen from comparing panels C and D on the left of Figure 5). In contrast, preference that decreases with the increasing osmolyte concentration implies a 'saturation' effect. In that case, increasing concentrations in the bulk barely affects the (already saturated) concentration in a local domain around the protein, meaning that the preference (being the ratio of the local and bulk concentrations) effectively decreases. As seen in Figure 5, for urea, these high-affinity regions correspond to the backbone and virtually all types of the side chains, as the preference function for the 7.0 M solution lies below the 3.5 M curve almost everywhere, except for the bulk solvent where the curves overlap by definition. For betaine, such high-affinity regions only exist at the basic side chains and at large distances (0.6–0.8 nm) from the protein, corresponding largely to the second solvation shell around the basic regions.

Analysis of interaction energies reveals the nature of osmolyte accumulation and exclusion

Recent theoretical considerations led to a conclusion that the overall nature of the stabilizing or destabilizing effect of osmolytes — either enthalpic or entropic — primarily depends on the contributions that dominate the effective osmolyte–solute interaction [53]. Hence, to investigate the nature of the driving forces behind the exclusion and accumulation of osmolytes, we first calculated the interaction enthalpies [$\Delta H_o(r)$ and $\Delta H_w(r)$] between a single osmolyte or water molecule and the environment, i.e. the protein and the rest of the solvent, as a function of the molecule's distance from the protein surface r (Supplementary Figure S8; see also captions in Figures 6 and 7 for details). From these profiles, we computed an effective interaction enthalpy profile by including the effect of solvent displacement, i.e. taking into account the fact that an approaching osmolyte molecule displaces a certain number of water and osmolyte molecules that would reside there otherwise. For betaine and urea, this effective enthalpy $\Delta H(r)$ was calculated as $\Delta H_o(r)(1 - y_o(r)) - q\Delta H_w(r)(1 - y_o(r))$, where $y_o(r)$ is the volume fraction of the osmolyte at a given distance r from the protein and q is the ratio of average molar volumes of osmolyte and water (4.17 in the case of betaine and 2.53 for urea). Subsequently, to relate the enthalpy changes to the actual distribution of the molecules around the protein, we computed the corresponding free energy profiles for protein–solvent association as $\Delta G(r) = -kT \ln \rho(r)$, where $\rho(r)$ is the protein–solvent radial distribution function. The translational contribution to the free energy was subtracted by employing a normalization scheme based on the surface area of the protein, as measured by a probe of radius r, which led to the free energy profiles that are flat at large distances from the protein surface. Eventually, by subtracting $\Delta H(r)$ from $\Delta G(r)$, we computed the entropic contribution to the association free energy [denoted as $-T\Delta S(r)$], which includes water-mediated

hydrophobic interactions and the abundance of solvent-binding sites at distance r that correspond to an average enthalpy of ΔH(r).

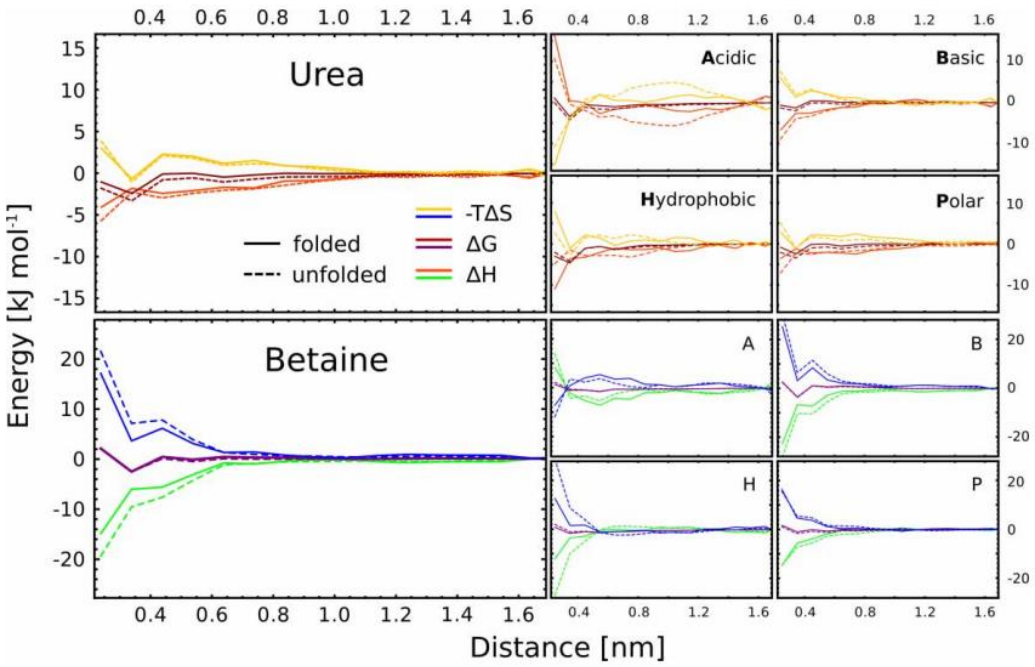

Figure 6. Δ*G*, Δ*H* and −*T*Δ*S* profiles for a single solvent molecule with respect to the protein surface.
The free energy (Δ*G*), enthalpy (Δ*H*) and entropy (−*T*Δ*S*) changes were computed for the 2.5 M betaine and 5.0 M urea solutions, as a function of the distance from the protein surface.

Figure 6 shows the resulting profiles for osmolyte molecules, computed as a function of the distance from the protein surface in the systems with intermediate osmolyte concentrations (2.5 M betaine and 5.0 M urea). To distinguish between different types of amino acid environments at the protein surface, the profiles were also determined with respect to acidic, basic, polar and hydrophobic residues and, separately, with respect to the backbone (Figure 7). The original $\Delta H_w(r)$ and $\Delta H_o(r)$ profiles used to compute ΔH(r) in Figures 6 and 7 are shown in Supplementary Figures S8 and S9.

As can be seen from Figures 6 and 7, approaching the protein surface is enthalpically favorable for a urea molecule, consistently for the backbone and all residue types — except for acidic side chains, where the high cost of desolvation disfavors direct interactions with the osmolyte (see also Supplementary Figure S8). For the protein as a whole, the average effective enthalpic gain of roughly −4–6 kJ/mol, arising due to H-bonding and van der Waals' interactions, remains favorable in terms of free energy despite the cost of displacing water molecules from the protein surface (~2.5 kJ/mol corresponding to ~2.5 water molecules replaced by a single urea molecule) and the loss of translational entropy (<3 kJ/mol in the range of concentrations studied). Therefore, the favorable direct interactions with the protein may be thought of as a major driving force behind the observed accumulation of urea at the protein surface.

To investigate these interactions in more detail and to examine their role in the unfolding process, we decomposed the solvation enthalpy change upon unfolding into individual contributions due to interactions between the solvent components and different types of residues. The results, shown in Supplementary Figures S10 and S11, clearly indicate that both electrostatic and van der Waals' interactions between the accumulated urea and the protein favor the unfolding process. As should be expected, this energy gain, seen in particular for the numerous hydrophobic and polar residues that become exposed to the solvent, is largely compensated by the loss of urea–water and urea–urea interactions (Supplementary Figure S12). The comparison with pure water (Supplementary Figure S10) shows, on the one hand, that the electrostatic contribution to the solvation enthalpy, related to the number and strength of protein–solvent hydrogen

bonds, is very similar regardless of the presence or concentration of urea. On the other hand, the van der Waals' interactions with the newly solvent-exposed side chains and backbone are much stronger for urea than for water and this difference results in the more negative solvation enthalpy change in the presence of urea. This observation supports the above argument that van der Waals' interactions rather than hydrogen bonds provide a critical enthalpic driving force for urea accumulation at the protein surface and hence for the urea-induced protein denaturation, which is consistent with previous reports [23,27,28,43].

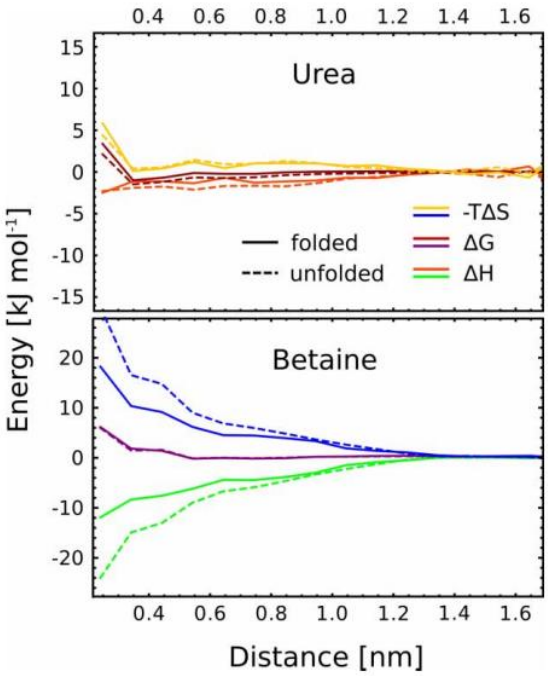

Figure 7. ΔG, ΔH and $-T\Delta S$ profiles for a single solvent molecule with respect to the protein backbone.
Free energy (ΔG), enthalpy (ΔH) and entropy ($-T\Delta S$) changes were for the 2.5 M betaine and 5.0 M urea solutions, as a function of the distance from the protein backbone.

Figure 6 further reveals that the enthalpic stabilization of the protein-bound urea is noticeably lower (by ~5 kJ/mol) in the vicinity of hydrophobic residues in the unfolded state and that, in this case, the broad minimum in the ΔH(r) curve is shifted by 0.4–0.6 nm toward the bulk solution. Even though the enthalpic driving force at hydrophobic patches favors the attraction of urea molecules toward the protein, the overall enthalpy change might not be sufficient to account for the preference of these regions for urea indicated by the ΔG(r) profile (see Figure 6). Indeed, a pronounced minimum in the −TΔS(r) curve (yellow dashed line in Figure 6H) coinciding with the free energy minimum strongly suggests that urea accumulation around hydrophobic patches is in part also entropically driven. In fact, as already suggested above, a urea-rich region adjacent to the protein surface can be thought of as a buffer to reduce the (mostly entropic) cost of exposing hydrophobic residues buried in the core to the solvent. Also consistent with this explanation is the fact that the interaction enthalpy for a water molecule has a broad minimum at slightly larger distances (0.4–0.8 nm) from hydrophobic residues in the unfolded state, in the urea-rich region around the protein (Supplementary Figure S8). This finding supports the picture in which accumulated urea molecules, by interacting favorably with the protein surface and, at the same time, with water, create a local environment that effectively weakens hydrophobic forces holding nonpolar groups together in the native protein structure.

Interaction analysis also sheds light on the molecular underpinnings of the protein-stabilizing effect of betaine, and possibly other methylamines. First, Figure 7 demonstrates that even though betaine does not preferentially associate with the exposed protein backbone (see also Figure 5), unexpectedly, this association is accompanied by a favorable enthalpy change (ΔH in the range of −20 to −10 kJ/mol). This

enthalpy gain is apparently more than offset by the positive −TΔS contribution, which makes the binding free energy unfavorable, supporting our claim that the exclusion of betaine results from the scarcity of binding sites capable of accommodating the ligand-like osmolyte molecule close to the backbone in an energetically optimal manner. Hence, our results point toward the first of two possible scenarios proposed above, where the exclusion mostly results from the effective repulsion due to an entropic factor that opposes protein–co-solvent association. However, while the canonical hard-sphere model assumes entirely steric nature of this repulsive force and hence a 'pure' excluded volume effect, in our description, the exclusion results mostly from the low availability of betaine-binding sites on the protein surface.

Accordingly, for the side chains, which are generally more accessible to the osmolyte molecules, no significant exclusion of betaine is observed in Figure 6 (flat free energy curve), even though in this case the corresponding enthalpy change is similar to (acidic residues) or smaller than (polar and hydrophobic residues) that for the backbone. It can be also seen from Figure 6 that the large minimum in the overall free energy profile of approximately −4 J/mol, corresponding to accumulation of betaine at ~0.35 nm, can be almost exclusively ascribed to the formation of salt bridges between the positively charged side chains and the carboxyl group of betaine.

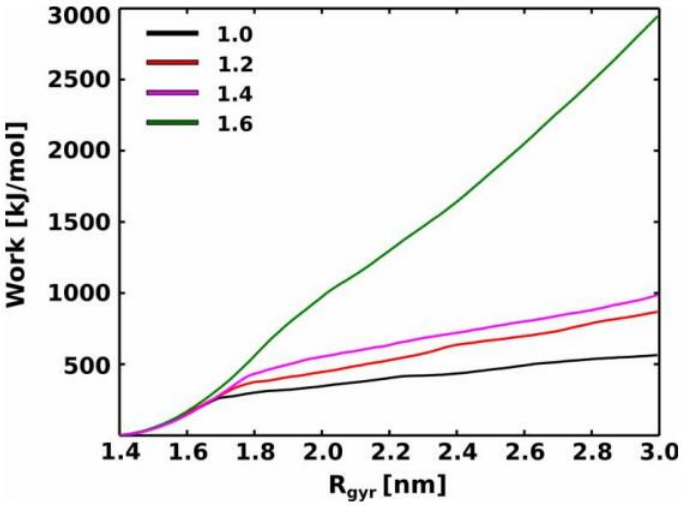

Figure 8. Changes in unfolding work upon the rescaling of partial charges in the betaine molecule.
The plot shows the amount of work required to unfold lysozyme in the presence of 5 M betaine with its partial charges scaled by a common factor ranging from 1.0 to 1.6, at the pulling speed of 5×10^{-6} nm ps^{-1}.

Aside from the dominant entropic contribution to the co-solvent-induced stabilizing effect, a growing body of evidence [46,54,81,90] points toward the existence of an enthalpic effect associated with the action of protecting osmolytes. This enthalpic contribution might arise due to changes in protein solvation, as already suggested by several researchers [81]. Indeed, in the H-bonding analysis, we found that betaine present as a co-solvent noticeably reduces the propensity of water to form hydrogen bonds with the protein, which is especially evident for the backbone, solvated almost exclusively by water. Supplementary Figure S9 provides additional insights into the observed reduced solvation effect, by showing that the enthalpic driving force for water–protein association is considerably smaller in the presence of betaine ($\Delta H_w \approx 0$) than in pure water ($\Delta H_w \approx -3$ to -2 kJ/mol). This difference indicates that the weaker hydrogen-bonding ability of water (or, more generally, the reduced activity of water) is caused by its strong interactions with betaine, consistent with the FTIR spectroscopy and molecular dynamics data showing a pronounced enhancement of the water structure upon the addition of betaine [74,91,92]. Interestingly, the analogous FTIR approach [21] and other experimental studies [23,28,87] have found that, unlike betaine, urea does not significantly affect the hydrogen-bonding network of water and is readily accommodated in liquid water structure. In agreement with these reports, the comparison of the original interaction enthalpy profiles ($H_w(r)$) for water

molecules in Supplementary Figure S9 shows that, in contrast with water-perturbing betaine, urea changes the energetics of interfacial water only very slightly ($\Delta\Delta H_w < 1$ kJ/mol).

Since the decreased solvation of the backbone and uncharged side chains in the presence of betaine necessarily disfavors the protein unfolding, the above findings support the notion that the betaine-induced stabilization is partially enthalpic in nature, as has been recently suggested [46,54,81,90]. Our data further indicate that the positive contribution to the enthalpy of unfolding is due to strong water–osmolyte interactions that reduce the ability of water molecules to solvate the newly exposed protein patches.

To additionally test the hypothesis about the enthalpic origin of protein stabilization by betaine, we scaled the partial charges of all betaine atoms by a common factor ranging from 1.0 to 1.6, and performed the mechanical unfolding simulations in 5 M betaine in the same manner as previously, at the lowest pulling speed of 5×10^{-6} nm ps^{-1}. As expected, the water-binding capacity increases with the polarity of the osmolyte molecule, as seen from the radial distribution functions in Supplementary Figure S13. Figure 8 shows that scaling up the charges led to a significant enhancement of the stabilizing effect of the co-solvent, as reflected in the increase in the unfolding work. This finding supports the notion that strong water binding might be partially responsible for the enthalpic contribution to the betaine-induced stabilization.

Conclusion

In this work, we studied the molecular origin of the perturbing effect of two osmolytes, urea and betaine, on the protein folding equilibrium. We simulated the mechanical unfolding of a lysozyme molecule in pure water and in aqueous solutions of both osmolytes, and found that our model correctly reproduced the stabilizing effect of betaine and the denaturing effect of urea, yielding larger and smaller values of unfolding work, respectively Subsequently, to analyze the effect of osmolytes on the calculated work of unfolding, we investigated the molecular determinants of protein stability in the studied solutions. In particular, we traced the formation of new protein–osmolyte and protein–water hydrogen bonds during the course of unfolding. We also quantitatively assessed the magnitude and spatial patterns of osmolyte exclusion and accumulation at the protein surface, and complemented these results with a detailed analysis of the enthalpy of interaction and its changes upon denaturation for individual components of the systems studied.

We observed that, in our model, urea accumulates in the vicinity of the protein, which according to most previously reported experimental and computational results is directly associated with the denaturing effect [13,40,42]. Intriguingly, however, we found that the concentration of urea increases not only at the protein surface, but rather remains elevated at distances of up to 1.0–1.5 nm from the protein, indicating the presence of a diffuse urea-rich solvation sphere around the lysozyme molecule. Also, while accumulating urea plays a major role in solvating the protein core that becomes exposed upon denaturation, the overall strength of newly formed protein–osmolyte and protein–water hydrogen bonds in urea solutions is in fact similar to that observed in pure water. This indicates that, contrary to certain recent claims [38], hydrogen bonding cannot account solely for the denaturing effect of urea. Instead, our data point to two other driving forces for urea-induced denaturation. First, we noted that the unfolded state is indeed stabilized by favorable direct interactions between urea molecules and the residues forming the protein core. As revealed by an analysis of the enthalpic terms and the accumulation patterns, this stabilization arises because urea forms favorable contacts with the protein in multiple spatial arrangements, regardless of the type of residues involved. Besides acting as both H-bond acceptors and donors, urea molecules also interact favorably with nonpolar residues by dispersion forces, stabilizing the unfolded conformation in which those residues are exposed to the solvent. Second, the results indicate that the diffuse urea-rich shell that forms around the protein is capable of accommodating well both water molecules and nonpolar protein residues, effectively screening the protein from the water-mediated hydrophobic force that drives protein folding.

In the case of betaine, we found that the osmolyte molecules are excluded from the protein surface, which is commonly believed to lead to the stabilization of proteins by betaine and other compatible osmolytes. We also observed that the exclusion is most pronounced in the vicinity of the backbone, in agreement with recent findings [39,40]. At the same time, the zwitterionic betaine molecules were found to accumulate near charged, mostly basic, residues, giving rise to an inhomogeneous and variable distribution on the protein surface.

Our data also indicate that even though the protein–betaine association is overall favorable in terms of enthalpy, it occurs infrequently, betaine forms very few new contacts with the protein upon unfolding and the newly exposed protein surface, consisting largely of the backbone and hydrophobic side chains, is mostly solvated by water. Based on our findings, we postulate that betaine — a rather bulky molecule with a large dipole moment — exhibits a ligand-like behavior, i.e. it can only be accommodated in an enthalpically favorable manner at relatively few binding places within the protein–solvent interface. This scarcity of binding sites in turn results in an effective exclusion of betaine from the protein backbone and uncharged side chains that is entropic in nature. Such a picture provides a molecular-level reinterpretation of the canonical entropydominated model of protein stabilization by protecting osmolytes. Moreover, our data suggest that the presence of betaine in a solution decreases the enthalpic driving force for protein hydration, since water molecules interact favorably with betaine in bulk solvent, as proposed in a recent study [47]. The resulting weakening of protein solvation (when compared with pure water) can give rise to an enthalpic contribution to the stabilizing effect of betaine, already reported by several researchers [46,54,81,90].

Funding

This research was partially supported by the PL-Grid Infrastructure and TASK Computational Center. This work was supported by the Polish National Science Centre (NCN) based on the decision (no. DEC-2013/11/B/NZ1/ 02258).

References

1 Mayor, U., Johnson, C.M., Daggett, V. and Fersht, A.R. (2000) Protein folding and unfolding in microseconds to nanoseconds by experiment and simulation. Proc. Natl Acad. Sci. USA 97, 13518–13522 doi:10.1073/pnas.250473497

2 Onuchic, J.N. and Wolynes, P.G. (2004) Theory of protein folding. Curr. Opin. Struct. Biol. 14, 70–75 doi:10.1016/j.sbi.2004.01.009

3 Daggett, V. (2006) Protein folding–simulation. Chem. Rev. 106, 1898–1916 doi:10.1021/cr0404242

4 Dill, K.A., Ozkan, S.B., Shell, M.S. and Weikl, T.R. (2008) The protein folding problem. Annu. Rev. Biophys. 37, 289–316 doi:10.1146/annurev.biophys.
37.092707.153558

5 Storey, K.B. (1997) Organic solutes in freezing tolerance. Comp. Biochem. Physiol. A Physiol. 117, 319–326 doi:10.1016/S0300-9629(96)00270-8

6 Gross, M. and Jaenicke, R. (1994) Proteins under pressure. The influence of high hydrostatic pressure on structure, function and assembly of proteins and protein complexes. Eur. J. Biochem. 221, 617–630 doi:10.1111/j.1432-1033.1994.tb18774.x

7 Yancey, P.H. (2001) Water stress, osmolytes and proteins. Amer. Zool. 41, 699–709 doi:10.1093/icb/41.4.699

8 Civera, T. (2003) Species identification and safety of fish products. Vet. Res. Commun. 27(Suppl 1), 481–489 doi:10.1023/B:VERC.0000014205.87859.ab

9 Khan, S.H., Ahmad, N., Ahmad, F. and Kumar, R. (2010) Naturally occurring organic osmolytes: from cell physiology to disease prevention. IUBMB Life
62, 891–895 doi:10.1002/iub.406

10 Bennion, B.J. and Daggett, V. (2003) The molecular basis for the chemical denaturation of proteins by urea. Proc. Natl Acad. Sci. USA 100,
5142–5147 doi:10.1073/pnas.0930122100

11 Street, T.O., Bolen, D.W. and Rose, G.D. (2006) A molecular mechanism for osmolyte-induced protein stability. Proc. Natl Acad. Sci. USA 103,
13997–14002 doi:10.1073/pnas.0606236103

12 Milev, S., Bosshard, H.R. and Jelesarov, I. (2005) Enthalpic and entropic effects of salt and polyol osmolytes on site-specific protein–DNA association:
the integrase Tn916–DNA complex. Biochemistry 44, 285–293 doi:10.1021/bi048907n

13 Canchi, D.R. and García, A.E. (2013) Cosolvent effects on protein stability. Annu. Rev. Phys. Chem. 64, 273–293 doi:10.1146/annurev-physchem-040412-110156

14 Bolen, D.W. and Rose, G.D. (2008) Structure and energetics of the hydrogen-bonded backbone in protein folding. Annu. Rev. Biochem. 77, 339–362 doi:10.1146/annurev.biochem.77.061306.131357
15 Canchi, D.R., Paschek, D. and García, A.E. (2010) Equilibrium study of protein denaturation by urea. J. Am. Chem. Soc. 132, 2338–2344 doi:10.1021/ja909348c
16 Bolen, D.W. (2004) Effects of naturally occurring osmolytes on protein stability and solubility: issues important in protein crystallization. Methods 34, 312–322 doi:10.1016/j.ymeth.2004.03.022
17 Ganguly, P., Hajari, T., Shea, J.-E. and van der Vegt, N.F.A. (2015) Mutual exclusion of urea and trimethylamine N-oxide from amino acids in mixed solvent environment. J. Phys. Chem. Lett. 6, 581–585 doi:10.1021/jz502634k
18 Timasheff, S.N. (1993) The control of protein stability and association by weak interactions with water: how do solvents affect these processes? Annu. Rev. Biophys. Biomol. Struct. 22, 67–97 doi:10.1146/annurev.bb.22.060193.000435
19 Brown, C.R., Hong-Brown, L.Q., Biwersi, J., Verkman, A.S. and Welch, W.J. (1996) Chemical chaperones correct the mutant phenotype of the ΔF508 cystic fibrosis transmembrane conductance regulator protein. Cell Stress Chaperones 1, 117–125 PMID: 9222597
20 Stumpe, M.C. and Grubmüller, H. (2007) Interaction of urea with amino acids: implications for urea-induced protein denaturation. J. Am. Chem. Soc. 129, 16126–16131 doi:10.1021/ja076216j
21 Panuszko, A., Bruź dziak, P., Zielkiewicz, J., Wyrzykowski, D. and Stangret, J. (2009) Effects of urea and trimethylamine-N-oxide on the properties of water and the secondary structure of hen egg white lysozyme. J. Phys. Chem. B 113, 14797–14809 doi:10.1021/jp904001m
22 Das, A. and Mukhopadhyay, C. (2009) Urea-mediated protein denaturation: a consensus view. J. Phys. Chem. B 113, 12816–12824 doi:10.1021/jp906350s
23 Zangi, R., Zhou, R. and Berne, B.J. (2009) Urea's action on hydrophobic interactions. J. Am. Chem. Soc. 131, 1535–1541 doi:10.1021/ja807887g
24 Horinek, D. and Netz, R. (2011) Can simulations quantitatively predict peptide transfer free energies to urea solutions? Thermodynamic concepts and force field limitations. J. Phys. Chem. A 115, 6125–6136 doi:10.1021/jp1110086
25 Bennion, B.J. and Daggett, V. (2004) Counteraction of urea-induced protein denaturation by trimethylamine N-oxide: a chemical chaperone at atomic resolution. Proc. Natl Acad. Sci. USA 101, 6433–6438 doi:10.1073/pnas.0308633101
26 Caballero-Herrera, A., Nordstrand, K., Berndt, K.D. and Nilsson, L. (2005) Effect of urea on peptide conformation in water: molecular dynamics and experimental characterization. Biophys. J. 89, 842–857 doi:10.1529/biophysj.105.061978
27 Stumpe, M.C. and Grubmüller, H. (2008) Polar or apolar — the role of polarity for urea-induced protein denaturation. PLoS Comput. Biol. 4, e1000221 doi:10.1371/journal.pcbi.1000221
28 Hua, L., Zhou, R., Thirumalai, D. and Berne, B.J. (2008) Urea denaturation by stronger dispersion interactions with proteins than water implies a 2-stage unfolding. Proc. Natl Acad. Sci. USA 105, 16928–16933 doi:10.1073/pnas.0808427105
29 Lee, S., Shek, Y.L. and Chalikian, T.V. (2010) Urea interactions with protein groups: a volumetric study. Biopolymers 93, 866–879 doi:10.1002/bip.21478
30 Canchi, D.R. and García, A.E. (2011) Backbone and side-chain contributions in protein denaturation by urea. Biophys. J. 100, 1526–1533 doi:10.1016/j.bpj.2011.01.028
31 Canchi, D.R., Jayasimha, P., Rau, D.C., Makhatadze, G.I. and García, A.E. (2012) Molecular mechanism for the preferential exclusion of TMAO from protein surfaces. J. Phys. Chem. B 116, 12095–12104 doi:10.1021/jp304298c
32 Dill, K.A. (1990) Dominant forces in protein folding. Biochemistry 29, 7133–7155 doi:10.1021/bi00483a001
33 Soper, A.K., Castner, E.W. and Luzar, A. (2003) Impact of urea on water structure: a clue to its properties as a denaturant? Biophys. Chem. 105, 649–666 doi:10.1016/S0301-4622(03)00095-4
34 Bandyopadhyay, D., Mohan, S., Ghosh, S.K. and Choudhury, N. (2013) Correlation of structural order, anomalous density, and hydrogen bonding network of liquid water. J. Phys. Chem. B 117, 8831–8843 doi:10.1021/jp404478y
35 Bandyopadhyay, D., Bhanja, K., Mohan, S., Ghosh, S.K. and Choudhury, N. (2015) Effects of concentration on like-charge pairing of guanidinium ions and on the structure of water: an all-atom molecular dynamics simulation study. J. Phys. Chem. B 119, 11262–11274 doi:10.1021/acs.jpcb.5b03064
36 Frank, H.S. and Franks, F. (1968) Structural approach to the solvent power of water for hydrocarbons: urea as a structure breaker. J. Chem. Phys. 48, 4746 doi:10.1063/1.1668057
37 Aastrand, P.O., Wallqvist, A. and Karlstroem, G. (1994) Molecular dynamics simulations of 2 m aqueous urea solutions. J. Phys. Chem. 98, 8224–8233 doi:10.1021/j100084a046
38 Rösgen, J., Pettitt, B.M. and Bolen, D.W. (2005) Protein folding, stability, and solvation structure in osmolyte solutions. Biophys. J. 89, 2988–2997 doi:10.1529/biophysj.105.067330
39 Auton, M., Marcelo, L., Holthauzen, F. and Bolen, D.W. (2007) Anatomy of energetic changes accompanying urea-induced protein denaturation. Proc. Natl Acad. Sci. USA 104, 15317–15322 doi:10.1073/pnas.0706251104
40 Auton, M., Rösgen, J., Sinev, M., Marcelo, L., Holthauzen, L.F. and Bolen, D.W. (2011) Osmolyte effects on protein stability and solubility: a balancing act between backbone and side-chains. Biophys. Chem. 159, 90–99 doi:10.1016/j.bpc.2011.05.012
41 Holthauzen, L.M.F., Rösgen, J. and Bolen, D.W. (2010) Hydrogen bonding progressively strengthens upon transfer of the protein urea-denatured state to water and protecting osmolytes. Biochemistry 49, 1310–1318 doi:10.1021/bi9015499
42 Guinn, E.J., Pegram, L.M., Capp, M.W., Pollock, M.N. and Record, M.T. (2011) Quantifying why urea is a protein denaturant, whereas glycine betaine is a protein stabilizer. Proc. Natl Acad. Sci. USA 108, 16932–16937 doi:10.1073/pnas.1109372108
43 Lee, M.-E. and van der Vegt, N.F.A. (2006) Does urea denature hydrophobic interactions? J. Am. Chem. Soc. 128, 4948–4949 doi:10.1021/ja058600r

44 Felitsky, D.J. and Record, M.T. (2004) Application of the local-bulk partitioning and competitive binding models to interpret preferential interactions of glycine betaine and urea with protein surface. Biochemistry 43, 9276–9288 doi:10.1021/bi049862t
45 Felitsky, D.J., Cannon, J.G., Capp, M.W., Hong, J., Wynsberghe, A.W.V., Anderson, C.F. et al. (2004) The exclusion of glycine betaine from anionic biopolymer surface: why glycine betaine is an effective osmoprotectant but also a compatible solute. Biochemistry 43, 14732–14743 doi:10.1021/bi049115w
46 Zou, Q., Bennion, B.J., Daggett, V. and Murphy, K.P. (2002) The molecular mechanism of stabilization of proteins by TMAO and its ability to counteract the effects of urea. J. Am. Chem. Soc. 124, 1192–1202 doi:10.1021/ja004206b
47 Ma, L., Pegram, L., Record, M.T. and Cui, Q. (2010) Preferential interactions between small solutes and the protein backbone: a computational analysis. Biochemistry 49, 1954–1962 doi:10.1021/bi9020082
48 Pieraccini, S., Conti, S., Chaurasia, S. and Sironi, M. (2013) Modelling the effect of osmolytes on peptide mechanical unfolding. Chem. Phys. Lett. 578, 138–143 doi:10.1016/j.cplett.2013.06.008
49 Macchi, F., Eisenkolb, M., Kiefer, H. and Otzen, D.E. (2012) The effect of osmolytes on protein fibrillation. Int. J. Mol. Sci. 13, 3801–3819 doi:10.3390/ijms13033801
50 Yancey, P., Burg, M. and Bagnasco, S.M. (1990) Effects of NaCl, glucose and aldose reductase inhibitors on cloning efficiency of renal cells. Am. J. Physiol. 258, 156–163
51 Asakura, S. and Oosawa, F. (1954) On interaction between two bodies immersed in a solution of macromolecules. J. Chem. Phys. 22, 1255 doi:10.1063/1.1740347
52 Sapir, L. and Harries, D. (2014) Origin of enthalpic depletion forces. J. Phys. Chem. Lett. 5, 1061–1065 doi:10.1021/jz5002715
53 Sapir, L. and Harries, D. (2015) Is the depletion force entropic? Molecular crowding beyond steric interactions. Curr. Opin. Colloid Interface Sci. 20,
3–10 doi:10.1016/j.cocis.2014.12.003
54 Politi, R. and Harries, D. (2010) Enthalpically driven peptide stabilization by protective osmolytes. Chem. Commun. (Camb) 46, 6449–6451 doi:10.1039/c0cc01763a
55 Gilman-Politi, R. and Harries, D. (2011) Unraveling the molecular mechanism of enthalpy driven peptide folding by polyol osmolytes. J. Chem. Theory Comput. 7, 3816–3828 doi:10.1021/ct200455n
56 Bandyopadhyay, D., Mohan, S., Ghosh, S.K. and Choudhury, N. (2014) Molecular dynamics simulation of aqueous urea solution: is urea a structure breaker? J. Phys. Chem. B 118, 11757–11768 doi:10.1021/jp505147u
57 Lai, B., Cao, A. and Lai, L. (2000) Organic cosolvents and hen egg white lysozyme folding. Biochim. Biophys. Acta, Protein Struct. Mol. Enzymol. 1543,
115–122 doi:10.1016/S0167-4838(00)00189-8
58 Vanommeslaeghe, K., Hatcher, E., Acharya, C., Kundu, S., Zhong, S., Shim, J. et al. (2010) J. Comput. Chem. 31, 671–690 PMID:19575467
59 Best, R.B., Zhu, X., Shim, J., Lopes, P.E.M., Mittal, J., Feig, M. et al. (2012) Optimization of the additive CHARMM all-atom protein force field targeting improved sampling of the backbone w, ψ and side-chain χ_1 and χ_2 dihedral angles. J. Chem. Theory Comput. 8, 3257–3273 doi:10.1021/ct300400x
60 Courtenay, E.S., Capp, M.W., Anderson, C.F. and Record, M.T. (2000) Vapor pressure osmometry studies of osmolyte−protein interactions: implications for the action of osmoprotectants in vivo and for the interpretation of 'osmotic stress' experiments in vitro . Biochemistry 39, 4455–4471 doi:10.1021/bi992887l
61 Jorgensen, W.L., Chandrasekhar, J., Madura, J.D., Impey, R.W. and Klein, M.L. (1983) Comparison of simple potential functions for simulating liquid water. J. Chem. Phys. 79, 926 doi:10.1063/1.445869
62 Mackerell, A.D., Feig, M. and Brooks, C.L. (2004) Extending the treatment of backbone energetics in protein force fields: limitations of gas-phase quantum mechanics in reproducing protein conformational distributions in molecular dynamics simulations. J. Comput. Chem. 25, 1400–1415 doi:10.1002/jcc.20065
63 Lindahl, E., Hess, B. and van der Spoel, D. (2001) GROMACS 3.0: a package for molecular simulation and trajectory analysis. J. Mol. Mod. 7, 306–317 doi:10.1007/s00894010004
64 Darden, T., York, D. and Pedersen, L. (1993) Particle mesh Ewald: an N·log(N) method for Ewald sums in large systems. J. Chem. Phys. 98,
10089–10092 doi:10.1063/1.464397
65 Essmann, U., Perera, L., Berkowitz, M.L., Darden, T., Lee, H. and Pedersen, L.G. (1995) A smooth particle mesh Ewald method. J. Chem. Phys. 103, 8577–8593 doi:10.1063/1.470117
66 Berendsen, H.J.C., Postma, J.P.M., van Gunsteren, W.F., DiNola, A. and Haak, J.R. (1984) Molecular dynamics with coupling to an external bath. J. Chem. Phys. 81, 3684–3690 doi:10.1063/1.448118
67 Hess, B., Bekker, H., Berendsen, H. and Fraaije, J. (1997) LINCS: a linear constraint solver for molecular simulations. J. Comp. Chem. 18, 1463–1472 doi:10.1002/(SICI)1096-987X(199709)18:12<1463::AID-JCC4>3.0.CO;2-H
68 Espinosa, E., Molins, E. and Lecomte, C. (1998) Hydrogen bond strengths revealed by topological analyses of experimentally observed electron densities. Chem. Phys. Lett. 285, 170–173 doi:10.1016/S0009-2614(98)00036-0
69 Humphrey, W., Dalke, A. and Schulten, K. (1996) VMD: visual molecular dynamics. J. Mol. Graph. 14, 33–38 doi:10.1016/0263-7855(96)00018-5
70 Shank, E.A., Cecconi, C., Dill, J.W., Marqusee, S. and Bustamante, C. (2010) The folding cooperativity of a protein is controlled by its chain topology. Nature 465, 637–640 doi:10.1038/nature09021

71 Yang, G., Cecconi, C., Baase, W.A., Vetter, I.R., Breyer, W.A., Haack, J.A. et al. (2000) Solid-state synthesis and mechanical unfolding of polymers of T4 lysozyme. Proc. Natl Acad. Sci. USA 97, 139–144 doi:10.1073/pnas.97.1.139
72 Tyrrell, H.J.V. and Kennerley, M. (1968) Viscosity B-coefficients between 5° and 20° for glycolamide, glycine, and N-methylated glycines in aqueous solution. J. Chem. Soc. A 2724–2728 doi:10.1039/J19680002724
73 Singh, M. and Kumar, A. (2006) Hydrophobic interactions of methylureas in aqueous solutions estimated with density, molal volume, viscosity and surface tension from 293.15 to 303.15 K. J. Solution Chem. 35, 567–582 doi:10.1007/s10953-005-9008-7
74 Bruz´dziak, P., Panuszko, A. and Stangret, J. (2013) Influence of osmolytes on protein and water structure: a step to understanding the mechanism of protein stabilization. J. Phys. Chem. B 117, 11502–11508 doi:10.1021/jp404780c
75 Panuszko, A., S´ miechowski, M. and Stangret, J. (2011) Fourier transform infrared spectroscopic and theoretical study of water interactions with glycine and its N-methylated derivatives. J. Chem. Phys. 134, 104–115 doi:10.1063/1.3567202
76 Lim, W.K., Rösgen, J. and Englander, S.W. (2009) Urea, but not guanidinium, destabilizes proteins by forming hydrogen bonds to the peptide group. Proc. Natl Acad. Sci. USA 106, 2595–2600 doi:10.1073/pnas.0812588106
77 Vanzi, F., Madan, B. and Sharp, K. (1998) Effect of the protein denaturants urea and guanidinium on water structure: a structural and thermodynamic study. J. Am. Chem. Soc. 120, 10748–10753 doi:10.1021/ja981529n
78 Zou, Q., Habermann-Rottinghaus, S.M. and Murphy, K.P. (1998) Urea effects on protein stability: hydrogen bonding and the hydrophobic effect. Proteins 31, 107–115 PMID: 9593185
79 Makhatadze, G.I. and Privalov, P.L. (1992) Protein interactions with urea and guanidinium chloride. J. Mol. Biol. 226, 491–505 doi:10.1016/0022-2836(92)90963-K
80 Rupley, J.A. (1964) The effect of urea and amides upon water structure. J. Phys. Chem. 68, 2002–2003 doi:10.1021/j100789a503
81 Ma, J., Pazos, I.M. and Gai, F. (2014) Microscopic insights into the protein-stabilizing effect of trimethylamine N-oxide (TMAO). Proc. Natl Acad. Sci. USA 111, 8476–8481 doi:10.1073/pnas.1403224111
82 Parsegian, V.A., Rand, R.P. and Rau, D.C. (2000) Osmotic stress, crowding, preferential hydration, and binding: a comparison of perspectives. Proc. Natl Acad. Sci. USA 97, 3987–3992 doi:10.1073/pnas.97.8.3987
83 Moeser, B. and Horinek, D. (2014) Unified description of urea denaturation: backbone and side chains contribute equally in the transfer model. J. Phys. Chem. B 118, 107–114 doi:10.1021/jp409934q
84 Capp, M.W., Pegram, L.M., Saecker, R.M., Kratz, M., Riccardi, D., Wendorff, T. et al. (2009) Interactions of the osmolyte glycine betaine with molecular surfaces in water: thermodynamics, structural interpretation, and prediction of m-values . Biochemistry 48, 10372–10379 doi:10.1021/bi901273r
85 Diehl, R.C., Guinn, E.J., Capp, M.W., Tsodikov, O.V. and Record, M.T. (2013) Quantifying additive interactions of the osmolyte proline with individual functional groups of proteins: comparisons with urea and glycine betaine, interpretation of m-values. Biochemistry 52, 5997–6010 doi:10.1021/bi400683y
86 Holehouse, A.S., Garai, K., Lyle, N., Vitalis, A. and Pappu, R.V. (2015) Quantitative assessments of the distinct contributions of polypeptide backbone amides versus side chain groups to chain expansion via chemical denaturation. J. Am. Chem. Soc. 137, 2984–2995 doi:10.1021/ja512062h
87 Funkner, S., Havenith, M. and Schwaab, G. (2012) Urea, a structure breaker? Answers from THz absorption spectroscopy. J. Phys. Chem. B 116, 13374–13380 doi:10.1021/jp308699w
88 Carr, J.K., Buchanan, L.E., Schmidt, J.R., Zanni, M.T. and Skinner, J.L. (2013) Structure and dynamics of urea/water mixtures investigated by vibrational spectroscopy and molecular dynamics simulation. J. Phys. Chem. B 117, 13291–13300 doi:10.1021/jp4037217
89 O'Brien, E.P., Dima, R., Brooks, B. and Thirumalai, D. (2007) Interactions between hydrophobic and ionic solutes in aqueous guanidinium chloride and urea solutions: lessons for protein denaturation mechanism. J. Am. Chem. Soc. 129, 7346–7353 doi:10.1021/ja069232+
90 Senske, M., Törk, L., Born, B., Havenith, M., Herrmann, C. and Ebbinghaus, S. (2014) Protein stabilization by macromolecular crowding through enthalpy rather than entropy. J. Am. Chem. Soc. 136, 9036–9041 doi:10.1021/ja503205y
91 Athawale, M.V., Dordick, J.S. and Garde, S. (2005) Osmolyte trimethylamine-N-oxide does not affect the strength of hydrophobic interactions: origin of osmolyte compatibility. Biophys. J. 89, 858–866 doi:10.1529/biophysj.104.056671
92 Athawale, M.V., Sarupria, S. and Garde, S. (2008) Enthalpy−entropy contributions to salt and osmolyte effects on molecular-scale hydrophobic hydration and interactions. J. Phys. Chem. B 112, 5661–5670 doi:10.1021/jp073485n